A Spot Weld Modeling and Application in Impact Simulation of Longitudinal Beam

Ye Yingtai[1], Peng Qian[1], Yang Jikuang[1], Wu Shenrong[2], Guo Jie[2]

1. State Key Laboratory of Advanced Design and Manufacture for Vehicle Body, Hunan University, Changsha, 410082; 2. Automobile Engineering Research Institute, Chery Automobile Co. Ltd, Wuhu

Abstract: The aim of the study is to investigate the use of FE spot weld model consisting of solid elements in the crash simulation of car structure connected by welding. Such model was established with the LS-DYNA software and it was applied for the crash FE simulation of longitudinal beam. The corresponding sled test using longitudinal beam was carried out to validate the spot weld finite element model. The failure behavior of spot weld, the deformation of longitudinal beam and the acceleration of the sled were compared between the simulation and test. The influence from the added mass and hourglass energy of the solid elements on the reliability was also evaluated in the simulations. The results from this study show that the proposed spot weld modeling methodology is accurate and reliable.

Key words: Crash Simulation, Spot Weld Modeling, Solid Element, Failure of Spot Weld

1 Introduction

Body-In-White structure of a car widely consists of hundreds of fabricated sheet metal parts joined together by spot welds. There are more than 5,000 spot welds in a car, so the car is a typical spot weld structure. It is found that the characteristics of spot weld have a significant effect on the crash safety of vehicles. With the Computer Assistant Engineering (CAE) analysis methods, which are frequently applied in crash simulations, it has a great significance to improve the accuracy of FE model particularly in simulation reliably of the spot weld connections.

The investigations, how to develop the model of spot weld, were performed by various researchers. Matzenmiller et al. [1] compared several one-dimensional (1D) spot weld models such as those using bar elements, rivet elements, rigid constraints, and discrete beam elements. They recommended the nonlinear discrete beam element model to be used in simulations of spot welds. Dreas [2] improved the accuracy of this model considering properties of surface nodes. In another study He et al. [3] used simple elements in form of rigid beams to create a spot weld model, and this model shows a good agreement with validation test of impact to thin-walled beam.

Considering the deformation of spot weld, the deformable beam elements were used in simulation with LS-DYLA [4]. In another study Madasamy et al. used two-node spring elements with 6 DOF at each node to model the spot weld, and presented the energy based failure criteria of spot weld. Their simulation results showed a better agreement with the test results [5]. Seeger et al. pointed out that the two-dimensional (2D) beam element model was unable to simulate the torsion behavior of spot weld in structures and recommend the solid element model [6]. In another study Xiang showed also that the simulation results of quasi-static collapse of hat thin-walled structures are better when solid element model is used to represent spot weld; especially in the case of non-spot weld failure [7].

Based on this literature review in the study we decided to use the solid elements model from LS-DYNA software in simulations of spot weld. This model was applied in the finite element crash simulation of longitudinal beam. To validate the spot weld model the corresponding sled test of impact to longitudinal beam was carried out. The failure behavior of spot weld, the deformation of longitudinal beam and the acceleration of the sled were compared between the simulation and test. The influence from the added mass and hourglass energy of the solid elements on the reliability was also evaluated in the simulation.

2 Simulation of the spot weld connection

In the macro level, the spot weld in the automotive structure consists of the metal sheets and weld nugget (Figure 1). The micro level of spot weld is shown in Figure 2. According to material properties, three regions can be identified in a spot weld: a weld nugget with cylindrical shape (region 1), a heat-affected zone (region 2) and basic metal sheet (region 3).

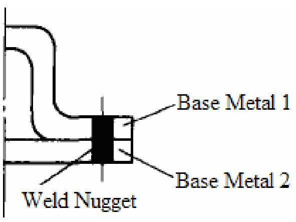

Figure 1. The sketch of typical spot weld

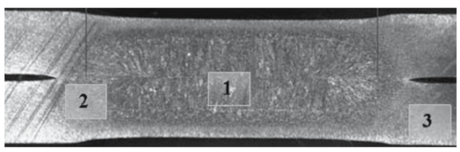

Figure 2. The micro level spot weld

Because the spot weld itself and the surrounding material properties had been changed in the process of welding due to the heat development [8]. In the spot weld finite element model developed in LS-DYNA, the base metal sheets were modeled using Belytschko-Tsay shell elements. Piecewise linear plastic constitutive model (MAT24) was selected to represent the material properties of metals. The material curves of the base metal sheets were gained via the quasi-static tensile tests. Ignoring the difference of properties of the heat-affected zone and weld nugget both zones were represented by a single solid element of constant strain type. The thickness of this element is the distance between two neutral surfaces of the base metal sheets; length is the weld nugget diameter. The material properties of weld nugget in LS-DYNA were defined using spot weld constitutive model (MAT100).

The mechanical properties between base metal and weld nugget were simulated by defining the contact between shell and solid element. This contact was treated as tied interface constraint by the keyword *CONTACT-TIED-SURFACE TO SURFACE. Established finite element model of spot weld is shown in Figure 3.

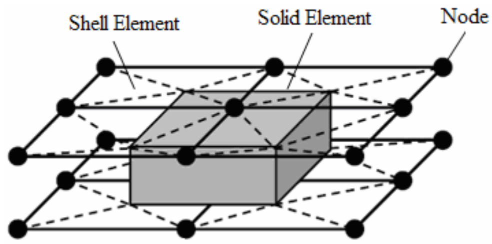

Figure 3. FE model of welding-spot

3 Simulation of spot weld failure

3.1. Spot Weld Failure Mode

There are two modes for spot weld failure: weld nugget button-pullout fracture and interfacial fracture. The button-pullout mode I is shown in Figure 4 (a), this fracture involves damage in the base material rather than through the fused region of the weld. A weld button forms because fracture develops along the periphery of the weld (i.e., within the heat affected zone - HAZ, or the base material). The button-pullout mode II is shown in Figure 4 (b), where a hole is produced in one of the sheets. The interface fracture mode is shown in Figure 4 (c), this is in not so common and also less desirable one. In this fracture mode a separation of the joined sheets occurs as a result of weld damage. Spot weld failure mode is affected by spot weld geometry, base metal and stress state. The hardness of weld nugget is usually higher than the base metal, such as the spot weld of DP600 steel. For this steel the weld nugget's hardness is 1.87 ~ 2.45 times higher than one of original steel. Therefore button-pullout fracture will occur more often than interfacial fracture in the area of spot weld when the high strength steel is used [9].

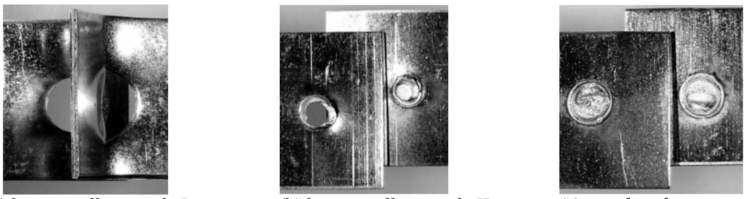

(a) button-pullout mode I (b) button-pullout mode II (c) interface fracture mode

Figure 4. The various types of welding-spot fracture according to [9]

In the current study we used this classification of weld failure modes in analysis of the test results.

3.2 Spot weld failure criterion definition

In the finite element simulation of the collision, there are many spot weld failure criterions described in the literature, such as combined load based criterion, stress and energy based criterion and so on. The two-dimensional combined load based failure criterion defined in term of normal and shear loads is the most commonly used.

Wang further developed this criterion and in one study showed that the rotation of metal around spot weld would develop the torque in it. Therefore, it would more accurate taking account of the spot weld torque in the combined load based failure criterion [10]. Therefore in current study we used the combined loads criterion including normal, shear and torsion loads as the spot weld failure. Failure criterion expressions are as follows:

$$\left(\frac{\max(f_n,0)}{F_n}\right)^2+\left(\frac{f_s}{F_s}\right)^2+\left(\frac{m_t}{M_t}\right)^2-1\geq 0 \qquad \text{(Equation 1)}$$

where f_n is the actual normal load considering the tensile force only; F_n is the critical normal load; f_s is the actual shear load, F_s is the critical shear load; m_t is the actual torque, M_t is the critical torque.

The forces and torque of the nodes of spot weld elements were calculated from in FE simulation. Once the actual load surface of the internal normal force, shear force and torque is above the critical surface according to Equation 1, the nodes of spot weld element will began to remove. When the nodes of spot weld element are completely removed, the constraint force between this element and shell element is completely released and the failure of spot weld occurs.

4 Effect of the mesh offset on the internal welds forces

The loads in the spot weld criterion expression are the internal weld forces. In the actual finite element model, the mesh elements of the base metal sheets were offset in the area of spot weld connection. The literature [11] pointed out that the internal weld forces used as the weld failure criteria must remain consistent regardless of relative placement of the weld to the master segments in order to successfully apply predictive weld failure. To study internal weld forces the KS-II tests were more and more widely used in recent years. Therefore, this we studied the effect of mesh offset on the internal weld forces using the KS-II numerical model. KS-II numerical model test is showed in Figure 5.

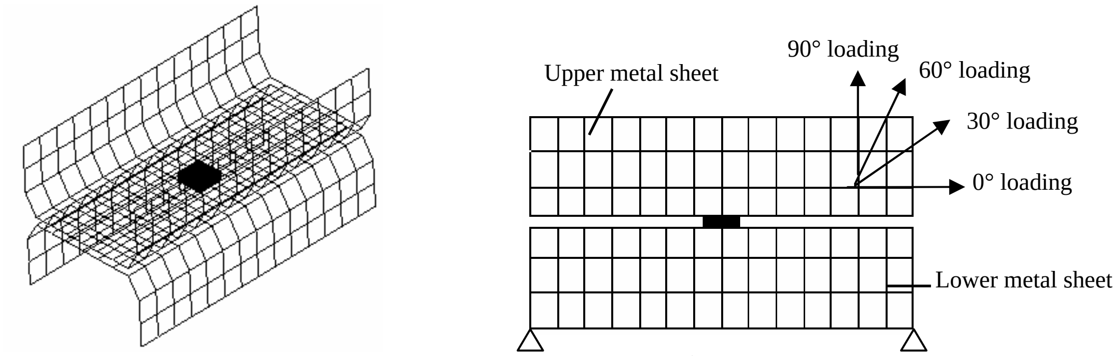

(a) Iso view (b) front view

Figure 5. KSⅡ-test numerical model

Figure 5 (b), The upper metal sheet was loaded with a force at various angles of 0°, 30°, 60° and 90° and loading speed of 5 mm/ms.The lower metal sheet was fixed using nodes constraint. A mesh offset between upper and lower shell element had been chosen in steps of 0%, 25%, 50%, 75%, 95% of one shell element as shown in Figure 6.

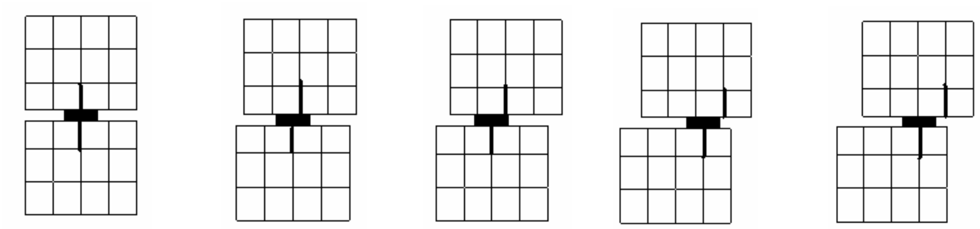

(a) 0% offset (b) 25% offset (c) 50% offset (d) 75% offset (e) 95% offset

Figure 6. The sketch of various mesh offset

In the case when the loading is applied at 0°, although only shear load was applied, the weld nugget was actually subjected to tensile force. In the 30° and 60° loading geometry, the weld nugget was subjected not only the tensile force but also shear force. In the 90° loading geometry, although only tensile load was applied, the weld nugget was actually subject to shear force. It could be seen from Figure 7, that the internal weld forces were basically same in the cases of different mesh offset. Therefore, the internal weld forces are unaffected by the mesh offset of the base metal sheets. The spot weld failure criteria is valid in all cases of different mesh offset. So, it was not necessary to consider the smaller mesh, and the modeling workload would be reduced.

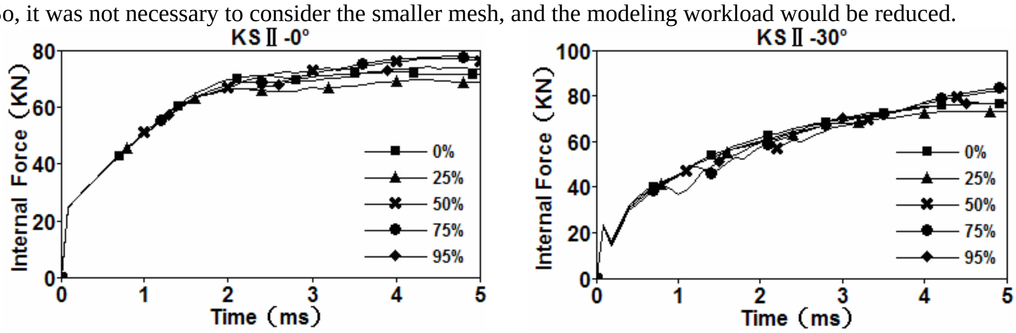

(a) the internal weld force-time curve in 0° loading (b) the internal weld force-time curve in 30° loading

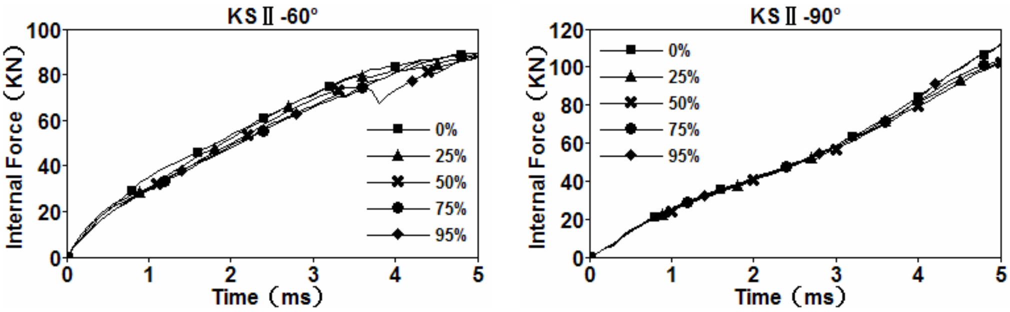

(c) the internal weld force-time curve in 0° loading (d) the internal weld force-time curve in 0° loading

Figure 7. The spot weld internal force of various mesh offset in KS-Ⅱ simulation

5 The simulation case and validation by sled test

5.1 Simulation case

The sled crash simulation was carried out using the model of longitudinal beam taken from certain domestic vehicle as shown in Figure 10. The total length of the studied beam was 470 mm. The two metal segments of the beam were connected using tailor-welded technology; the anterior segment was 250 mm. The thickness of the inside and outside metal sheets of DP600 of anterior segment was 1.8 mm. The thickness of the inside and outside metal sheets of SAPH440 for hind segment was 2.2 mm. The length of auxiliary energy absorption tube of B180H1 was 300 mm and the thickness was 2 mm. The material properties of various steels were gained via quasi-static (0.001 / s) tensile test. The specific material parameters are shown in Table 1.

Table1. Material parameters

Material	Density [kg/mm^3]	Young's Modulus [Gpa]	Poisson's ratio	Yield stress [Mpa]	Tensile stress [Mpa]	C [1/ms]	P	Plastic strain of Material failure [×100%]
DP600	7.8×10^{-6}	210	0.3	420	650	1.8	3	0.55
SAPH440	7.8×10^{-6}	210	0.3	340	550	8	5	0.60
B180H1	7.8×10^{-6}	210	0.3	250	340	0.7	3	0.63

The spot weld model presented previously was applied in the longitudinal beam finite element model. The length of solid spot weld element was set to 6.5 mm according to the average diameter of the spot welds in specimen. The yield stress of the spot weld was determined by the Equation 2:

$$\frac{H_{VW}}{\sigma_{SW}} = \frac{H_{VU}}{\sigma_{SU}} \qquad \text{Equation 2}$$

where: H_{VW} is the Vickers hardness of spot weld, σ_{SW} is the yield strength of spot weld, H_{VU} is the Vickers hardness of metal, σ_{SU} is the yield strength of metal. When $H_{VW} / H_{VU} = 2.24$ according to Marya and Wang [9], the yield strength of spot welds was calculated as 940 MPa.

In order to obtain the failure load of the spot weld in tension, we carried out three box-tensile tests of spot welds of DP600 sheets (see Figure 8). The diameter of weld nugget was 6.5 mm. The force-displacement curves are shown in Figure 9. As it can be seen from this figure the average spot weld failure force is 15 kN. Therefore, the normal failure load of spot welds for the anterior segment of the longitudinal beam in the simulation was set to 15 kN. Based on the literature [12] the spot weld normal load can be estimated as 60% ~ 75% of the shear load. Therefore for the simulation we choose the shear failure load for this steel as 21 kN. The torque was set to 35 kN based on the experience. The spot weld failure for the hind segment of the longitudinal beam was not considered.

Figure 8. Tensile test for a DP600 welding-spot

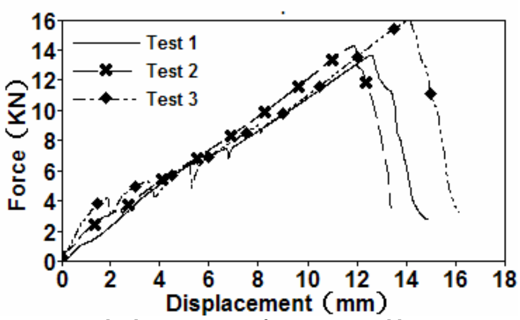

Figure 9. Force-displacement curve for a DP600 welding-spot in tensile test

5.2 Validation procedure by sled test

In order to validate the spot weld finite element model, the corresponding sled impact test was carried out. We used the longitudinal beam specimen as shown in Figure 10. The beam consisted of two parts A that was hind segment and B that was anterior segment. Both parts were tailor-welded. On this figure, C marks are showing the induced slot, the spot welds on the flange of tailor-welded anterior segment are marked via black circles. The configuration of sled test is shown in Figure 11. The longitudinal beam specimen was installed in the front of sled. To prevent total collapse of the beam there were two assisted energy-absorption tubes installed on each side of it. The metal blocks were installed at the middle of sled to match vehicle mass of 1020 kg. Accelerometer was installed at the middle of sled frame. To record the process of longitudinal beam deformation and the spot welds failure the high-speed video cameras were installed at top, left and right of crash spot. There was not possible to have a camera below the sled so the image of the spot weld failure behavior on the lower flange was not recorded The sled impacted the fixed rigid barrier at the initial speed of 13.9 mm/ms.

To verify the accuracy of the spot weld finite element model, we decided to compare the failure time of spot weld, the deformation of longitudinal beam and the acceleration of the sled between the simulation and test. Due to the small thickness of solid elements, mass scaling will lead to too much added mass in the simulation. The large deformation of these elements would cause hourglass energy. If added mass or hourglass energy is too much, the simulation results would be unauthentic. Our target was to keep added mass within 5% of the total mass and the hourglass energy within 5% of the total internal energy.

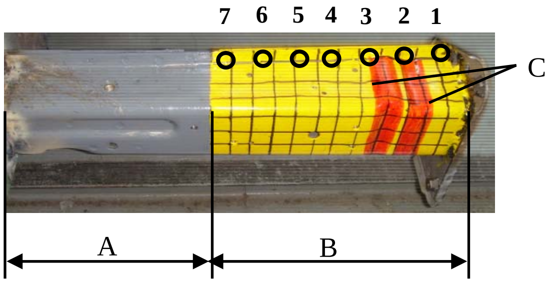

Figure 10. Longitudinal beam specimen

Figure 11. Configuration of sled test for longitudinal beam impact

6 Result and discussion

6.1 Comparison of spot weld failure

The analysis of the spot weld failure mainly focused on the upper flange. The observation from the videos and verified with the ocular examination of impacted specimen had shown that the spot welds on the upper flange were fractured with button-pullout type, while the spot welds at the hind segment were not fractured. The initial deformation of the longitudinal beam started from the second induced slot, it caused fracture of the spot weld 3#. With the deformation of the metal sheets the spot welds in succession failed. In the test and simulation there were almost the same failure times of spot welds from 1# to 7# (Table 2).

Table2. The failure time of spot welds

Failed Spot Weld ID		1	2	3	4	5	6	7
Failure time of Spot weld [ms]	Test	5	7	4	8	8	11	13
	Simulation	6.3	6.8	3.6	7.7	8.5	11.4	14.4

6.2 Comparison of the longitudinal beam deformation

In Figure 12, the deformation mode, fold location and number were similar between the simulation and the test. The deformation length of longitudinal beam was almost same (See table 3).

(a) the final deformation in test

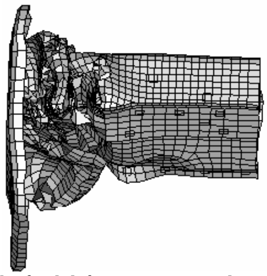

(b) the final deformation in simulation

Figure 12. Deformation of the longitudinal beam after impact

Table3. Deformation result of the longitudinal beam

	Test	Simulation
The length of the beam after impact [mm]	180	166
The length of tailor-welded anterior segment after impact [mm]	40	36
The length of energy absorbing tube after impact [mm]	180	166

6.3 Comparison of the sled acceleration

The form of sled acceleration curves was similar between the simulation and test as shown in Figure 13. The acceleration became zero at the same time, the peak values and its occurrence were also in a good agreement.

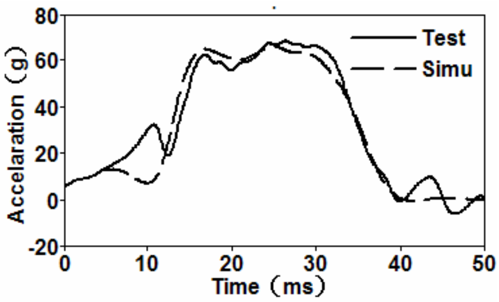

Figure 13. Acceleration curves of the sled

6.4 Added mass of the solid elements and the analysis of the hourglass energy

As shown in Figure 14, with the increasing number of spot weld failure, the added mass of spot welds is decreased in succession from 0 ms to 14.4 ms The added mass is almost constant after 14.4 ms. From the high-speed videos we could see that the spot welds at the tailor-welded anterior segment completely failed at 14.4 ms. The added mass of the spot welds was in normal range in the entire simulation. The time history of hourglass energy of spot welds is shown in Figure 15. The hourglass energy of the solid elements is within the normal range in the entire simulation. So the effect of the hourglass energy could be ignored.

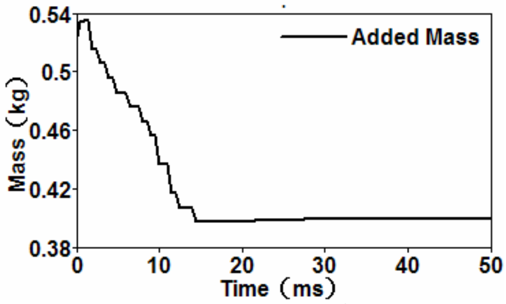

Figure 14. Added mass of spot weld

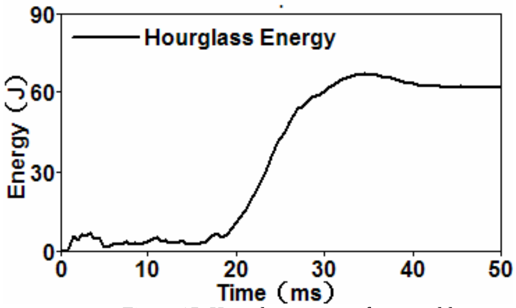

Figure 15. Hourglass energy of spot weld

7 Conclusions

The comparison of failure of spot welds, deformation of longitudinal beam and the sled acceleration had shown that the developed spot welds finite element model using solid elements could accurately simulate the connection metal sheets and the spot welds failure. The added mass and hourglass energy caused by the solid element were in normal range so that the simulation results were reliable. Therefore, the spot welds model developed in the study can be applied to simulate such connections in whole vehicle crash models.

Reference

[1] Matzenmiller A., Sehweizerhof. K., Rust, W. (1994). Joint Failure Modeling in Crashworthiness Analysis. 2nd International LS-DYNA3D Conference. San Francisco.

[2] Dreas K V. (1998). Welding-spot Modeling for Crash Computations. Requirements and New Functionalities in Ls-dyna，Version 940. 5th International Ls-dyna Users Conference. Michigan.

[3] He W., Zhang W.G.., Zhong Z.H. (2006). New Finite Element Modeling Technique for Spot-welds of Auto body in Vehicle Dynamic Simulation Automotive Engineering. 28(1):81-84. (In Chinese).

[4] LS-DYNA Keyword User's Manual. Version 970. 2003.

[5] Madasamy, C., Tyan, T., Faruque, O. (2004). Determination of Spot Weld Modeling Parameters from Test Data for Finite Element Crash Simulation. SAE: Paper number 2004-01-0692.

[6] Seeger F., Feucht M., Frank Th., Keding B., Haufe A., (2005) A. Haufe. An Investigation on Welding-spot Modeling for Crash Simulation with LS-DYNA. 4th LS-DYNA User Forum. Bamgerg.

[7] Xiang Y. J. (2004) Finite Element Analysis and Optimization on Crashworthiness of Vehicle Body's Thin-walled Metal Structures. MS Thesis, Department of Automotive Engineering, Tsinghua University, Beijing.

[8] Lamouroux E. H. J., Coutellier D., Doelle N., Kuemmerlen P. (2007) Detailed model of spot-welded joints to simulate the failure of car assemblies. Int J Interact Des Manuf, 1:33–40.

[9] Marya, M., Wang, K. (2006). Tensile-Shear Forces and Fracture Modes in Single and Multiple Weld Specimens in Dual-Phase Steels. Journal of Manufacturing Science and Engineering, 128:287~298.

[10] P. Wung, T. W., A. Ourchane, W. Stewart and M. Jie. (2001) Failure of Welding-spots under In-plane Static Loading .Testal Mechanics. 41(1): 100~106.

[11] Skye M., Nutwell E., (2007) Spot-weld Failure Prediction using Solid Element Assemblies. 6th European LS-DYNA Users Conference.

[12] Xie Y. Q., Fang R. H., Lei Y. C. (2003) Distribution Method of Welding Spot on Automobile Girder using Crash Simulation. Transactions of the China Welding Insutitution. 24(1): 73~76. (In Chinese)